THE EFFECTS OF HORIZONTAL DENSITY GRADIENTS AND SLOPING BOUNDARIES ON THE PROPAGATION OF INERTIAL-INTERNAL WAVES

By Christopher N.K. Mooers
Department of Oceanography
Oregon State University, U.S.A.

INTRODUCTION -

Strong horizontal density gradients, or, equivalently, baroclinic-geostrophic flows, occur in many regions of the ocean, especially in oceanic fronts and boundary currents. Inertial-internal waves, i.e., waves under the influence of both the earth's rotation and the ocean's density stratification, are also prominent in coastal regions. Thus, it is of interest to determine the influence of horizontal density gradients and sloping boundaries on inertial-internal waves.

THE GOVERNING EQUATION -

The following assumptions are made :

1) the fluid is inviscid, non-diffusive, and incompressible.

2) the wave motion is linear.

3) the effects of the horizontal component of the Coriolis force and of the earth's sphericity are negligible; hence, it is valid to neglect the latitudinal variations of the Coriolis force and to use Cartesian coordinates.

4) the Boussinesq approximation is valid.

5) the mean flow, $\underline{\bar{V}}$, consists of an axial component oriented along the y-axis and the cross-stream components are neglected, i.e., $\underline{\bar{V}} = (0, \bar{v}, 0)$.

6) the mean flow is in hydrostatic and geostrophic equilibrium, i.e., the so-called thermal wind relation applies :

(*) Presently a NATO Postdoctoral Fellow · in the Department of Oceanography - University of Liverpool - Liverpool 3, England.

$$f\bar{v}_z = \frac{-g\bar{\rho}_x}{\rho_o} = M^2 = -sN^2 \ ,$$

where f is the vertical component of the Coriolis force,

g is the gravitational acceleration oriented along the z-axis, which is positive upwards,

ρ_o is the space-time-averaged mass density,

$s = \left|\frac{dz}{dx}\right|_{\bar{\rho}}$ is the vertical slope of an isopycnal in the vertical plane transverse to the mean flow and the x-axis is the horizontal coordinate axis normal to the mean flow,

$N^2 = \frac{-g\bar{\rho}_z}{\rho_o}$ is the square of the Väisälä-Brunt frequency, and

M^2 ⟵ is the horizontal analogue of N^2.

The above assumptions yield the following system of equations :

the momentum equations :

$$(1.1)\quad D(u) - f\,v = -\pi_x \ ,$$

$$(1.2)\quad D(v) + (f+\bar{v}_x)\,u + \bar{v}_z w = -\pi_y \ ,$$

$$(1.3)\quad D(w) - b = -\pi_z$$

the equation of continuity :

$$(1.4)\quad u_x + v_y + w_z = 0$$

the bouyancy equation :

$$(1.5)\quad D(b) + M^2 u + N^2 w = 0,$$

where $v = (u,v,w)$ is the fluctuating component of the velocity;

$D(\ ) = (\ )_t + \bar{v}(\ )_y$ is the total time derivative;

$\tilde{\rho}$ is the total mass density field, which is partitioned such that

$$\tilde{\rho} = \rho_o + \bar{\rho}(x,z) + \rho(x,z,t),$$

where $\bar{\rho}$ and $\rho << \rho_o$;

$\pi = \dfrac{\rho+\rho_o gz}{\rho_o}$ is the fluid pressure, ρ, per unit mass density, which incorporates the Boussinesq approximation;
and

$b = \dfrac{-g\rho}{\rho_o}$ is the bouyancy.

Postponing discussion of the full three-dimensional case, the quasi-two-dimensional case, i.e., where $(\ )_y = 0$ though v is not neglected, is first examined. In this case, a stream function, ψ, exists such that $u = -\psi_z$ and $w = \psi_x$. Assuming simple harmonic time dependence, i.e., all fluctuating variables proportional to $e^{i\sigma t}$, system (1) reduces to the governing equation, (2) :

$$(2a) : (N^2-\sigma^2)\psi_{xx} - 2M^2\psi_{xz} - (\sigma^2-\sigma_f^2)\ \psi_{zz} = 0$$

or

$$(2b) : \psi_{xx} + (\lambda_1+\lambda_2)\ \psi_{xz} + \lambda_1\lambda_2\psi_{zz} = 0$$

or

$$(2c) : \psi_{\eta\zeta} = C(\psi_\eta, \psi_\zeta) ,$$

where $\sigma_f^2 = f(f+v_x)$ is the square of the effective inertial frequency,

$$\lambda_1, \lambda_2 = \frac{-M^2 \pm [M^4+(N^2-\sigma^2)(\sigma^2-\sigma_f^2)]^{\frac{1}{2}}}{(N^2-\sigma^2)}$$

are the slopes of the characteristics,

η, ζ are the characteristic coordinates,

$C(\psi_\eta, \psi_\zeta)$ is a function of ψ_η, ψ_ζ, and the partial derivatives of λ_1 and λ_2 and vanishes if λ_1 and λ_2 are constant.

Equation (2) is exact under the constraint that $\bar{\rho}$ and $\bar{v}$ satisfy the thermal wind relation.

From (2), the y-component of the vorticity, $\omega^{(y)}$, is

$$\omega^{(y)} = u_z - w_x$$

$$= -\nabla^2 \psi$$

$$= -\left[\frac{N^2}{\sigma^2}\,\psi_{xx} + \frac{2M^2}{\sigma^2}\,\psi_{xz} + \frac{f^2}{\sigma^2}\,\psi_{zz}\right] .$$

Hence, f, M, and N all contribute to the rotationality of the motion. In a similar way, they also contribute to the effective potential energy of the wave.

QUALITATIVE PROPERTIES -

A thorough discussion of the qualitative properties is given in Mooers (1970b) and only a limited discussion is given below. First, equation (2) is spatially hyperbolic for $\sigma_l < \sigma < \sigma_u$, i.e., for σ in the passband for free waves, where

$$\sigma_l^2 \approx \sigma_f^2 - s^2 N^2$$

and

$$\sigma_u^2 \approx N^2(1+s^2)$$

under the assumption that $\sigma_f^2 << N^2$. Since, for western and eastern boundary currents, $s \sim 10^{-3}$ to 10^{-2}, $N^2 \sim 10^{-5}$ to 10^{-4} $\sec^{-2}$, and $\sigma_f^2 \sim 10^{-8}$ $\sec^{-2}$, then $\sigma_u^2 \approx N^2$ and σ_l^2 can be appreciably less than σ_f^2. Hence, horizontal density gradients are likely to be far more important for low frequency than for high frequency inertial-internal waves. In fact, when $\sigma_f^2 = s^2 N^2$, $\sigma_l^2 = 0$ without approximation. Thus, the passband extends to

the zero frequency for $|s| = s_c = \frac{\sigma_f}{N}$, the critical slope, and to imaginary frequencies for $|s| > s_c$. Insight into the significance of s_c is obtained from the examination of the frontal Richardson number, FRN :

$$FRN = \frac{N^2}{(v_z)^2}$$

$$= \frac{f^2}{s^2 N^2}$$

$$\xrightarrow[s \to s_c]{} \frac{1}{(1+R_o)} ,$$

where $R_o = \frac{\bar{v}_x}{f}$ is the Rossby number, with sign, for $\bar{v}$. Thus, as s becomes critical, FRN becomes critical unless $R_o \simeq -1$; in which case the flow is barotropically unstable anyway.

Second, the passband divides into the three sub-bands summarized below for $s > 0$:

anomalously low frequencies (a.l.f.)	normal frequencies (n.f.)	anomalously high frequencies (a.h.f.)
$\sigma_l < \sigma \leq \sigma_f$	$\sigma_f \leq \sigma \leq \sigma_N$	$\sigma_N \leq \sigma < \sigma_u$
$\lambda_1 > 0$	$\lambda_1 > 0$	$\lambda_1 < 0$
$\lambda_2 > 0$	$\lambda_2 < 0$	$\lambda_2 < 0$, where $\sigma_N = N$.

The a.l.f. and a.h.f. are anomalous in two senses :

1) the fact of their existence,

and

2) the signs of λ_1 and λ_2 are the same; thus, all "wave beams" are oriented upwards in the a.l.f. and downwards in the a.h.f.

It also follows that $|\lambda_1| \neq |\lambda_2|$ except for $\sigma = \sigma_l$ or σ_u. Alternatively, the dispersion curves, Figure 1, imply distortion of the phase and group velocities for up-going and down-going "wave fronts" when $s \neq 0$. (Note : "wave fronts" and "wave beams" are orthogonal for inertial-internal waves.) It is necessary to realize that σ_f, σ_N, and s, and thus σ_l and σ_u, vary spatially in a frontal zone or baroclinic flow. Hence, when $s \neq 0$, not only is the passband altered but refractive effects, as indicated by the asymmetrization and variation of the slopes of the characteristics, occur as well. The refractive effects lead to phenomena termed frontal-blocking, frontal-trapping, and beam-splitting, c.f. Mooers (1970b).

Third, the primary effect of sloping boundaries on inertial-internal waves is summarized by the criticality, T, of the bottom slope, m :

$$T = \frac{-\lambda_2 + m}{(\lambda_1 - m)} ,$$

where $m \geq 0$ has been assumed. The amplification of wave amplitude and that of wave number upon reflection from a sloping boundary are proportional to T. There are three cases for T (Sandstrom, 1966) :

1) $T > 1$, subcritical or transmissive bottom slope;

2) $T < 1$, supercritical or reflective bottom slope;

and

3) $T \to \infty$, critical bottom slope, a degenerate case.

It is straightforward to prove that $T(s) < T(0)$ for $s > 0$ and $\sigma < N$ or $s < 0$ and $\sigma > N$. Hence, the criticality is reduced for σ in either the a.l.f. or n.f. when the slope of the bottom and that of the isopycnals have the same sign; the converse is true for σ in the a.h.f.

THE SOLUTION FOR CONSTANT COEFFICIENTS -

In the case of constant coefficients, equation (2c) becomes :

$$\phi_{\eta\zeta} = 0 \ ,$$

where $\eta = z - \lambda_1 x$ is the upgoing characteristic and $\zeta = z - \lambda_2 x$ is the downgoing characteristic. The general solution is then

$$\phi = \frac{1}{(\lambda_1 - \lambda_2)} \left[\lambda_1 F(\zeta) - \lambda_2 F(\eta)\right] \cos(\sigma t)$$

$$+ \left[G(\zeta) - G(\eta)\right] \cos(\sigma t + \Phi) \ ,$$

where F and G are the Cauchy, or initial, data which have at least piecewise continuous derivatives of the first order. Alternatively,

$$\phi = I\,U(\eta;t) + I\,D(\zeta;t) \ ,$$

where

$$I\,U = \frac{-1}{(\lambda_1 - \lambda_2)} \left[\lambda_2 F(\eta)\cos(\sigma t) + G(\eta)\cos(\sigma t + \Phi)\right.$$

is the upgoing Riemann invariant and

$$I\,D = \frac{1}{(\lambda_1 - \lambda_2)} \left[\lambda_1 F(\zeta)\cos(\sigma t) + G(\zeta)\cos(\sigma t + \Phi)\right.$$

is the downgoing Riemann invariant. The boundary conditions need only be applied to complete the solution, but, first, the geometry of the problem is examined.

A fundamental horizontal wavelength, L, exists only for waves with σ in the n.f. For uniform depth, H_o,

$$L(s) = \frac{H_o}{\lambda_1} + \frac{H_o}{(-\lambda_2)}$$

$$= \left[\frac{\lambda_1 - \lambda_2}{-\lambda_1 \lambda_2} \right] H_o$$

$$= \frac{[s^2 \mu^2 + \lambda_o^2]^{\frac{1}{2}}}{\lambda_o^2} \; 2H_o$$

$$\geqq L(0) = \frac{2H_o}{\lambda_o} \; ,$$

where

$$\lambda_o = \left[\frac{\sigma^2 - \sigma_f^2}{N^2 - \sigma^2} \right]^{\frac{1}{2}}$$

and

$$\mu = \frac{N^2}{(N^2 - \sigma^2)} \; .$$

Thus, for $s \neq 0$, the fundamental horizontal wavelength is increased regardless of the sign of s. Figure 2 illustrates the geometry of the limiting characteristics over a fundamental wavelength and the field of lines of constant phase, which shows zones of relative acceleration and retardation of wave fronts. In a similar fashion, for a subcritical, uniformly sloping bottom boundary, a fundamental horizontal wavelength, L_n, exists for a denumerable infinity of geometrically similar, contiguous sectors, $\{R_n;\ n : \text{interger}\}$, where

$$L_1(s) = \frac{H}{\lambda_1} \frac{(\lambda_1 - \lambda_2)}{(m - \lambda_2)}$$

$$= \left[\frac{-\lambda_2}{-\lambda_2 + m} \right] L(s)$$

$$\leqq L(s) \; ,$$

$$L_n(s) = (\gamma^{-1}\, T(s))^{1-n}\, L_1(s)\ ,$$

and

$$\gamma = -\frac{\lambda_2}{\lambda_1}\ .$$

Note : $L_n(s) \xrightarrow[n \to \infty]{} 0$ for the subcritical case.

When

$$s = 0,\ L_1(0) = \left[\frac{\lambda_o}{\lambda_o + m}\right] L(0),\ \gamma = 1,$$

and

$$L_n(0) = (T(0))^{1-n}\, L_1(0).$$

Figure 3 is analogous to Figure 2 and is for the case $s = 0$ and $m \neq 0$. Again, there are zones of relative acceleration and retardation of wave fronts over an effective wavelength. The case of $s \neq 0$ and $m \neq 0$ is an obvious generalization of Figures 2 and 3.

Since a fundamental wavelength exists, it is natural to expect the existence of a set of normal modes. In fact,

$$\psi \sim S = \sum_n a_n(t)\, c_n(x,z) + \sum_n b_n(t)\, s_n(x,z),$$

where

$$c_n(x,z) = \cos\left[\frac{k_n}{\lambda_2}(\zeta + H_o) - \cos\left(\frac{k_n}{\lambda_1}(\eta + H_o)\right)\right],$$

$$s_n(x,z) = \sin\left[\frac{k_n}{\lambda_2}(\zeta + H_o)\right] - \sin\left[\frac{k_n}{\lambda_1}(\eta + H_o)\right],$$

and

$$k_n = \frac{2\pi n}{L(s)}\ ,\ n : \text{integer}\ .$$

(The rigid boundary condition, i.e., $\psi = 0$ at $z = 0$ and $z = H_o$, has been imposed for simplicity.) Each mode is a strict (strong)

solution of (2) and the boundary conditions and has continuous partial derivatives of all orders. Yet, because ϕ has discontinuous first order normal derivatives across $\eta = -H_o, \zeta = 0$, etc.., ϕ is the general (weak) solution and S does not converge to ϕ. Further, when $s \neq 0$, the normal modes are non-separable in x and z, and they are not orthogonal over the interval $-H_o \leq z \leq 0$. Hence, it is awkward to expand the Cauchy data in terms of the normal modes. Similar effects occur in the case $s = 0$ and $m \neq 0$, where the discontinuous derivatives are due to the discontinuity in the bottom slope at the junction of a region of uniform depth and one of uniform bottom slope. Thus, several reasons have been presented for continuing with the analysis of the general solution.

The general solution will be constructed for the case $s \neq 0$ and $m \neq 0$. Again, rigid boundary conditions are applied for simplicity. They are now applied at $z = 0$ and $z = -H_o + mx$, $x \geq 0$. The solution for R_1 is constructed, and then the generalization to R_n follows by geometrical similarity. Several equivalent ways of carrying out the calculation have been found. The simplest and most concise is given below. First it is useful to recognize that each R_n has seven sub-sectors, I, II, ..., VII, in each of which the solution has a distinctive form. Referring to Figure 3 for the definition of the sub-sectors, writing the solution for each sector in terms of its Riemann invariants, and applying the boundary conditions sequentially to determine the unknown Riemann invariants, the solution for R_1 is written as

$$\phi_I = IU_I(\eta) + ID_I(\zeta) = IU(\eta) + ID(\zeta),$$

where IU and ID are as defined earlier and the time dependence is implicit;

$$\phi_{II}\ IU_{II}(\eta) + ID_{II}(\zeta) = IU(\eta) - IU(-\nu^{-1}\zeta)$$

$$\phi_{III} = IU_{III}(\eta) + ID_{III}(\zeta) = - ID[-(1+T)H_o - T\eta] + ID(\zeta)$$

$$\psi_{IV} = IU_{IV}(\eta) + ID_{IV}(\zeta) = -ID[-(1+T)H_o - T\eta] - IU(-\gamma^{-1}\zeta)$$

$$\psi_{V} = IU_{V}(\eta) + IF_{V}(\zeta) = -ID[-(1+T)H_o - T\eta]$$

$$+ID[-(1+T)H_o + \gamma^{-1}T\zeta]$$

$$\psi_{VI} = IU_{VI}(\eta) + ID_{VI}(\zeta) = IU\{\gamma^{-1}[(1+T)H_o + T\eta]\} - IU(-\gamma^{-1}\zeta)$$

and

$$\psi_{VII} = IU_{VII}(\eta) + ID_{VII}(\zeta)$$

$$= IU\{\gamma^{-1}[(1+T)H_o + T\eta]\} + ID[-(1+T)H_o + \gamma^{-1}T\zeta] .$$

It is a simple matter to verify ψ_{VII}; since

$$\psi_{VII}\Big|_{x=L_1} = IU(\gamma^{-1}T\ z) + ID(\gamma^{-1}T\ z),$$

$$\text{where } -\nu T^{-1} H_o \leq z \leq 0 ,$$

then $\psi_{VII}|_{x=L_1} \sim \psi_I|_{x=0}$, differing only in the fact that the argument of ψ_{VII} has been fractionally stretched in an amount inversely proportional to the fractional reduction in depth between $x = 0$ and $x = L_1$. For R_2, the solution is constructed in an analogous fashion, using ψ_{VII} as the new ψ_I. The generalization to the solution in R_n is then obvious.

THE THREE-DIMENSIONAL CASE -

A ray theory has been applied to the three-dimensional case in Mooers (1970b). A wave number vector, $\underline{k} = (k,l,m)$, and the intrinsic, or Doppler-shifted frequency, $\sigma = \sigma_o - \bar{v}_1$, where σ_o is the wave frequency, are introduced. Only the principal results are summarized below :

1) $$\frac{dk}{dt} = \bar{v}_x l \ ,$$

$$\frac{dl}{dt} = 0 \ ,$$

$$\frac{dm}{dt} = \bar{v}_z l \ ,$$

$$\frac{d\sigma_o}{dt} = 0 \ ,$$

and

$$\frac{d\sigma}{dt} = - \left[c_g^{(x)} \bar{v}_x + c_g^{(z)} \bar{v}_z \right] l \ ,$$

where t is travel time of a wave packet along a ray path, the group velocity is

$$\underline{c}_g = \left(c_g^{(x)}, c_g^{(y)}, c_g^{(z)} \right) \ ,$$

and the mean flow is assumed time independent.

2) Hence, l and σ_o are invariant, while $k \to \bar{v}_x t$ and $m \to \bar{v}_z t$ for large t <u>if</u> the ray-path-averaged $\bar{v}_x$ and $\bar{v}_z$ are non-vanishing. It is a consequence of this result that

$$\underline{c}_g \xrightarrow[t \to \infty]{} (0, \bar{v}, 0)$$

and, thus, that $\frac{d\sigma}{dt} \xrightarrow[t \to \infty]{} 0$ i.e., σ has a limiting value.

Further, <u>k</u> is turned into the vertical plane transverse to the mean flow and is oriented such that

$$\left. \frac{dz}{dx} \right|_\theta = \frac{-\theta_x}{\theta_z}$$

$$= \frac{-k}{m}$$

$$= \frac{-\bar{v}_x}{\bar{v}_z}$$

$$= \frac{dz}{dx}\Big|_{\bar{v}} \quad , \quad \text{i.e., the lines of constant phase,}$$

0, essentially coincide with the isotachs of $\bar{v}$. This result implies that the lines of constant phase tend to "wrap" themselves around the core of a geostrophic flow and to converge to the center of the core. Thus the group and phase velocities are also orthogonal, a basic property of inertial-internal waves, in the limit of large t.

3) The limiting value, σ_∞, of σ can be readily evaluated. In fact,

$$\sigma_\infty^2 = \left[\frac{N^2(\bar{v}_x)^2 - 2M^2\bar{v}_x\bar{v}_z + \sigma_f^2(\bar{v}_z)^2}{(\bar{v}_x)^2 + (\bar{v}_z)^2}\right]^{\frac{1}{2}} .$$

If $\bar{v}_x = 0$, $\sigma_\infty = f$; if $\bar{v}_z = 0$, $\sigma_\infty = N$.

Alternatively, with $\lambda = \frac{dz}{dx}\Big|_{\bar{v}}$,

$$\sigma_\infty^2 = \frac{N^2}{(1+\lambda^2)}\,(\lambda^2 + 2\lambda s + S_c^2)$$

and $\sigma^2 < 0$ if $|S| > |S_c|$ and $|\lambda+S| < (S^2-S_c^2)^{\frac{1}{2}}$.

Again, a supercritical isopycnal slope is a necessary condition for wave instability.

SUMMARY -

The Three-dimensional case can be employed to evaluate the significance of the quasi-two-dimensional case (l=0). If $l \neq 0$, the wave is refracted into the transverse in any event, and the intrinsic frequency is shiffted to a limiting value.Thus, for a frontal zone or geostrophic flow, a wave, in the case of $l = 0$, encounters, in a sense, an "open window", even though refractive effects in the transverse plane may still significantly affect the propagation of the waves. Though the limit of $t \rightarrow \infty$ is farfetched, and though the other idealizations employed deviate significantly from nature, the theoretical evidence is mounting for the existence of significant interactions between inertial-internal waves and geostrophic flows. The most important question remains open : is there appreciable energy exchange between inertial-internal waves and "mean" flows ?

BIBLIOGRAPHY -

MOOERS, Christopher N.K.(1970a) :
The Interaction of an Internal Tide with the Frontal Zone in a Coastal Upwelling Region. Ph.D.Thesis, Oregon State University, Corvallis, Oregon, 480 numb. leaves.

MOOERS, Christopher N.K.(1970b) :
The Effects of Horizontal Density Gradients on the Propagation of Inertial-Internal Waves. Geophysical Fluid Dynamics (submitted).

SANDSTROM, Helmuth(1966) :
The Importance of Topography in Generation and Propagation of Internal Waves. Ph.D.Thesis, University of California, San Diego, California, 105 numb.leaves.

LIST OF FIGURE CAPTIONS -

Figure 1. Dispersion Diagram (k>0)

downgoing and upgoing waves — — — , s = 0 ;

downgoing wave — . — . — . — , s > 0 ;
and
upgoing wave ———————— , s > 0 .

Figure 2. Wave Structure (s>0,m=0)

a. Geometry of the Characteristics

— . — . — . — , s = 0, m = 0 ;

and — — — — —, s > 0, m = 0 .

b. Lines of Constant Phase

———————— , s > 0, m = 0.

Figure 3. Wave Structure (s=0,m>0)

a. Geometry of the Characteristics

— — — — , s = 0, m > 0.

b. Lines of Constant Phase

———————— , s = 0, m > 0.

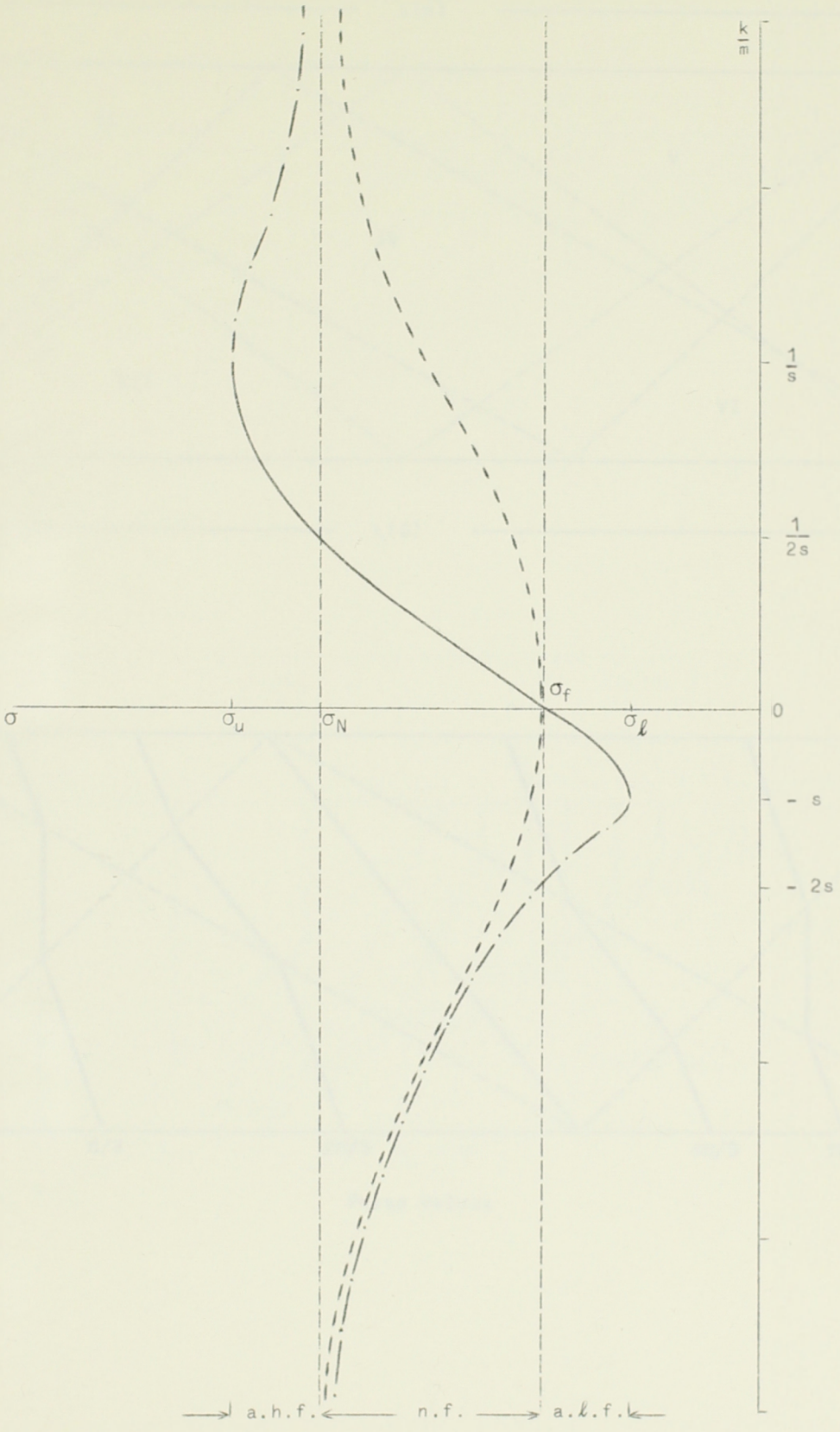

Fig. 1.

a.

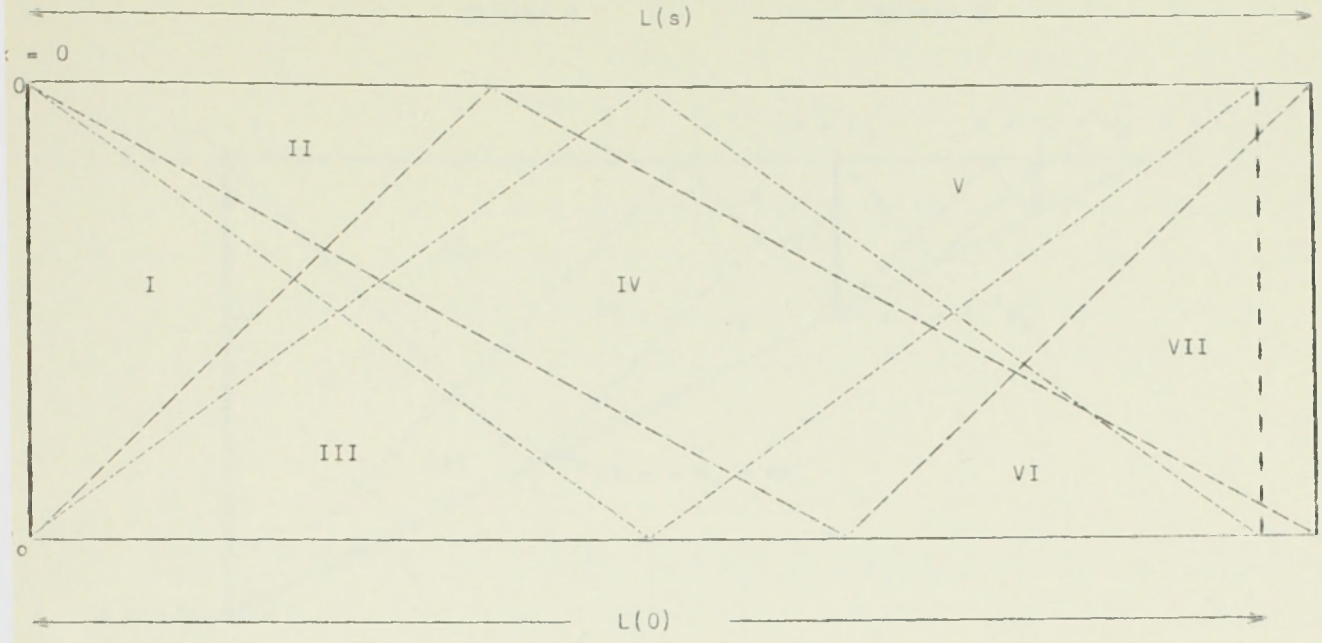

b.

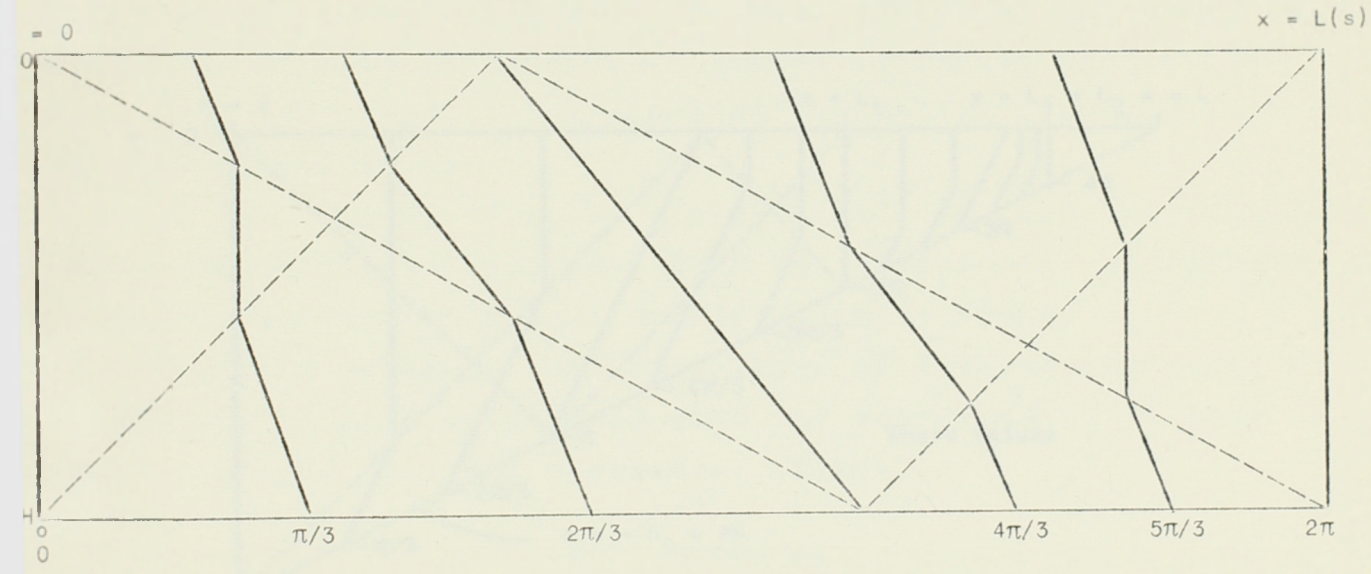

Phase Values

Fig. 2.

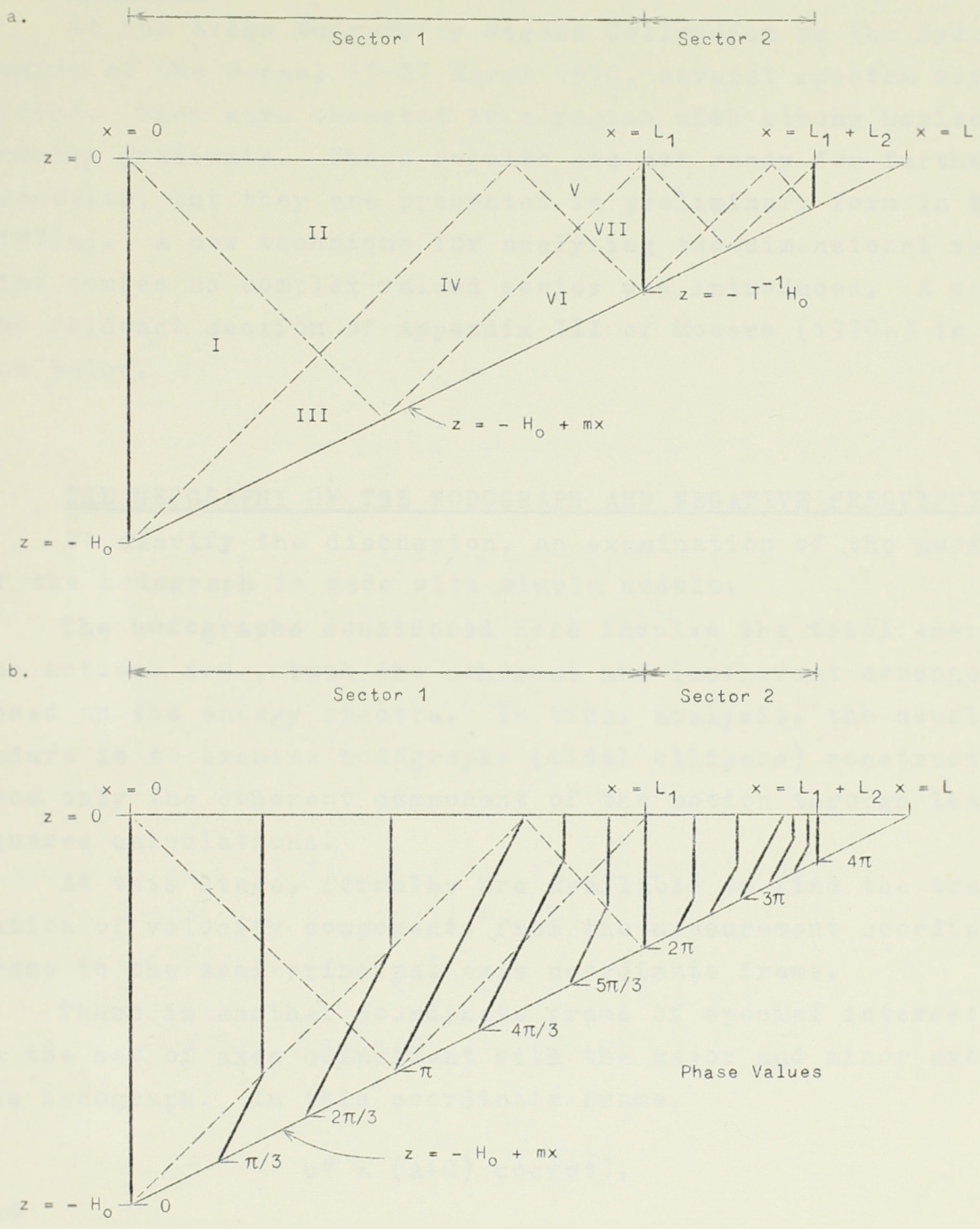
a.
Sector 1
Sector 2
x = 0
x = L1
x = L1 + L2
x = L
z = 0
I
II
III
IV
V
VI
VII
z = - T^-1 H0
z = - H0 + mx
z = - H0
b.
Sector 1
Sector 2
x = 0
x = L1
x = L1 + L2
x = L
z = 0
π/3
2π/3
π
4π/3
5π/3
2π
3π
4π
Phase Values
z = - H0 + mx
z = - H0
0

Fig. 3.

APPENDIX -

At the Liège University Second Colloquium on the Hydrodynamics of the Ocean, 17-20 March 1970, several spectra were displayed. They were observed in a region with strong horizontal density gradients. These results are not ready for further publication, but they are presented in preliminary form in Mooers (1970a). A new technique for analyzing two-dimensional velocity time series as complex-valued series was introduced. A copy of the relevant section of Appendix III of Mooers (1970a) is included below.

THE GEOGRAPHY OF THE HODOGRAPH AND NEGATIVE FREQUENCIES -

To clarify the discussion, an examination of the geography of the hodograph is made with simple models.

The hodographs considered here involve the total energy of the motion, i.e., both the coherent and incoherent components, based on the energy spectra. In tidal analysis, the usual procedure is to examine hodographs (tidal ellipses) constructed from only the coherent component of the motion through least squares calculations.

At this stage, formulae are available to find the transformation of velocity components from the measurement coordinate frame to the semi-principal axis coordinate frame.

There is another coordinate frame of special interest; it is the set of axes coincident with the major and minor axes of the hodograph. In this coordinate frame,

$$u'' = (A+C)\cos(\sigma t).$$

and

$$v'' = (A-C)\sin(\sigma t) ,$$

where A and C are amplitude factors. A and C can assume any non-negative, finite value. The eccentricity, ε , is $\varepsilon = A/C$ or C/A,

whichever is less than one. Since, in the semi-principal axis coordinate system,

$$P_{u'u'} = P_{v'v'} = \frac{P_{u''u''}+P_{v''v''}}{2}$$

$$= \frac{1}{2}\,(A^2+C^2)\ ,$$

the radius, R_o, of the hodograph along the semi-principal axes is $R_o = (A^2+C^2)^{1/2}$. By inspection,

$A = C$ gives rectilinear motion along the x"-axis,

$A = -C$ gives rectilinear motion along the y"-axis,

$C = 0$ gives anticlockwise circular motion,

$A = 0$ gives clockwise circular motion,

and

$A > C$ gives anticlockwise elliptical motion,

while

$C > A$ gives clockwise elliptical motion.

Thus, A is the amplitude of the anticlockwise component of the motion, while C is the amplitude of the clockwise component. The characterizing property of the ellipse-axes coordinate system is that $P_{u''v''} = 0$. The rotation from the (u,v) to the (u",v") velocity components through the angle θ_1 is then given by

$$\theta_1 = \frac{-1}{2}\,\tan^{-1}\left[\frac{2P_{uv}}{P_{vv}-P_{uu}}\right]\ ,$$

or

$$\theta_1 = \theta_o \pm \frac{\pi}{4}\ .$$

The component energy spectra in the ellipse-axes coordinate system are of special significance :

$$P_{u''u''} = \frac{P_{uu}+P_{vv}}{2} - \cos(2\theta_1)\frac{[P_{vv}-P_{uu}]}{2} + P_{uv}\sin(2\theta_1)$$

$$= \frac{P_{uu}+P_{vv}}{2} - \sin(2\theta_o)\frac{[P_{vv}-P_{uu}]}{2} - P_{uv}\cos(2\theta_o)$$

$$= \frac{P_{uu}+P_{vv}}{2} \pm \max P_{uv}$$

and, similarly,

$$P_{v''v''} = \frac{P_{uu}+P_{vv}}{2} \mp \max P_{uv} ,$$

which demonstrates that the Reynolds stress spectrum is related to the eccentricity of the hodograph. It is recognized that $P_{u''u''}$ and $P_{v''v''}$ are the eigenvalues of the real (or, even) part of the spectral matrix, thus they represent the squares of the lengths of the ellipse semi-axes, as they must.

There is an efficient means for solving for the amplitude and eccentricity of the hodograph from the spectral values : since

$$P_{u''u''} = \frac{(A+C)^2}{2}$$

and

$$P_{v''v''} = \frac{(A-C)^2}{2} ,$$

then

$$A \pm C = \sqrt{P_{uu}+P_{vv}+2 \max P_{uv}} = G$$

and

$$A \mp C = \sqrt{P_{uu}+P_{vv}-2 \max P_{uv}} = H ,$$

thus

$$\varepsilon = \frac{G-H}{G+H} .$$

Several properties of the hodograph can be deduced from the preceding formulae and model :

i) $J_1 = P_{uu} + P_{vv} = A^2 + C^2$,

ii) $J_2 = Q_{uv} = \frac{1}{2}(A^2-C^2)$,

($Q_{uv} = 0$ for $\varepsilon = 1$, i.e., for rectilinear motion)

iii) $J_3 = P_{uu}P_{vv} = (P_{uv})^2 = \frac{1}{4}(A+C)^2(A-C)^2 = (J_2)^2$, in the case of a single sinusoid), and

iv) $\max P_{uv} = [P_{uv}^2 + \frac{1}{4}(P_{vv}-P_{uu})^2]^{1/2}$

$= |AC|$, thus

$P_{uv} = 0$ for $\varepsilon = 0$, i.e., for circular motion.

An Example Hodograph. The geography of the hodograph is illustrated in Figure 4 for the following model. In the measurement coordinates, take

$$u = C \cos \sigma t + D \sin \sigma t$$

and

$$v = E \cos \sigma t + F \sin \sigma t ;$$

then

$$P_{uu} = \frac{1}{2}(C^2+D^2)$$

$$P_{vv} = \frac{1}{2}(E^2+F^2)$$

$$P_{uv} = \frac{1}{2}(CE+DF)$$

and

$$Q_{uv} = \frac{1}{2}(CF-DE).$$

For a quantitative example, take

$$C = \sqrt{3}, \quad D = 1/2 , \quad E = -1, \quad F = \sqrt{3/2} ;$$

a.

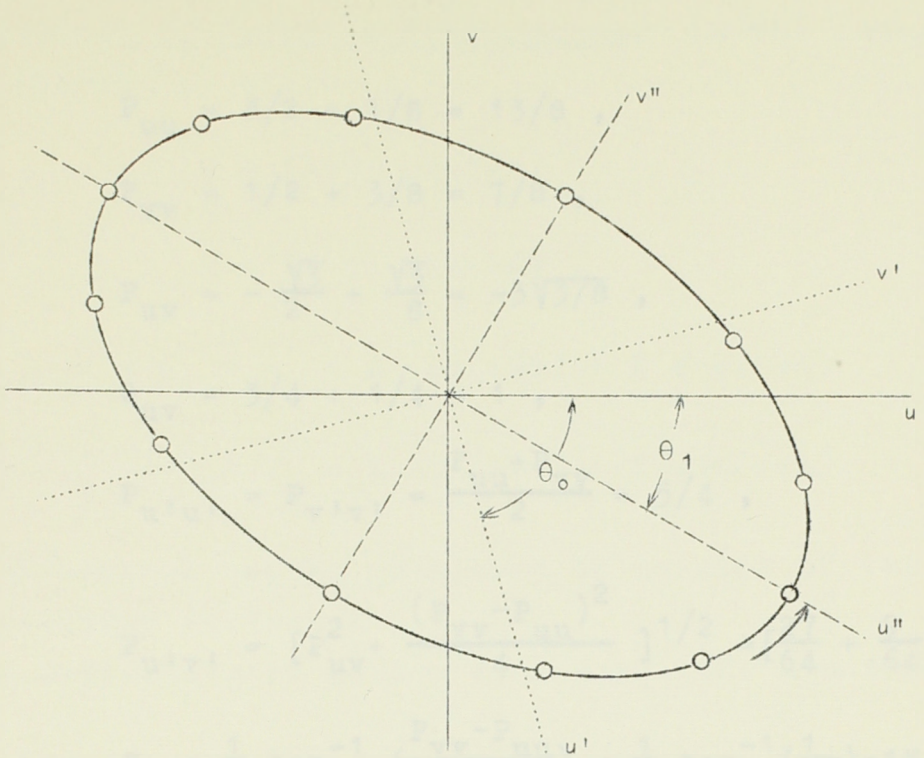

b.

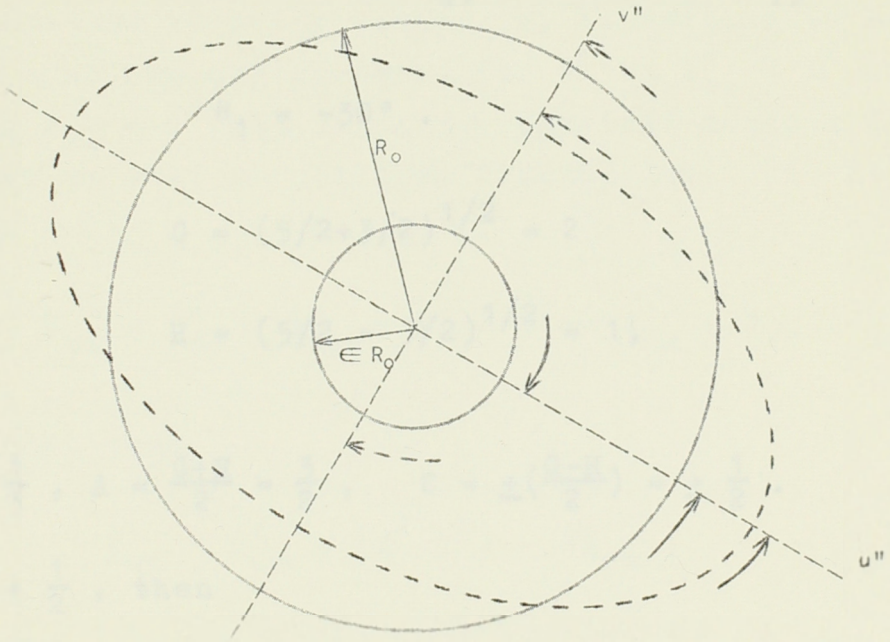

Fig. 4.- The geography of the hodograph.

a. The hodograph

(u,v) : geographic coordinates; (u',v') : semi-principal axes coordinates; (u",v") : ellipse-axes coordinates.

b. Decomposition of the hodograph into clockwise and anticlockwise components.

then

$$P_{uu} = 3/2 + 1/8 = 13/8 ,$$

$$P_{vv} = 1/2 + 3/8 = 7/8 ,$$

$$P_{uv} = -\frac{\sqrt{3}}{2} + \frac{\sqrt{3}}{8} = -3\sqrt{3/8} ,$$

$$Q_{uv} = 3/4 + 1/4 = 1 ,$$

$$P_{u'u'} = P_{v'v'} = \frac{P_{uu}+P_{vv}}{2} = 5/4 ,$$

$$P_{u'v'} = [P_{uv}^2 + \frac{(P_{vv}-P_{uu})^2}{4}]^{1/2} = [\frac{27}{64} + \frac{9}{64}]^{1/2} = 3/4 ,$$

$$\theta_0 = \frac{1}{2} \tan^{-1} (\frac{P_{vv}-P_{uu}}{2P_{uv}}) = \frac{1}{2} \tan^{-1}(\frac{1}{\sqrt{3}}) = 15^\circ ,$$

and

$$\theta_1 = -30^\circ .$$

Since

$$G = (5/2+3/2)^{1/2} = 2$$

and

$$H = (5/2 - 3/2)^{1/2} = 1,$$

then

$$\varepsilon = \frac{1}{3} , \quad A = \frac{G+H}{2} = \frac{3}{2} , \quad C = \pm(\frac{G-H}{2}) = \pm \frac{1}{2} .$$

Choose $C = + \frac{1}{2}$, then

$$u'' = (A+C) \cos(\sigma t) = 2 \cos (\sigma t)$$

and

$$v'' = (A-C) \sin(\sigma t)$$

$$= 1 \sin (\sigma t).$$

The Concept of Negative Frequencies. In the coordinates of the ellipse-axes, since

$$u = (A+C)\cos(\sigma t)$$

and

$$v = (A-C)\sin(\sigma t) ,$$

then

$$u = u^{+} + u^{-} = A\cos(+\sigma t) + C\cos(-\sigma t)$$

and

$$v = v^{+} + v^{-} = A\sin(+\sigma t) + C\sin(-\sigma t).$$

Thus, the hodograph can be conceived to consist of two counter-rotating velocity vectors :

i) An anticlockwise motion with amplitude A and frequency $+\sigma$, and

ii) A clockwise motion with amplitude C and frequency $-\sigma$.

The complex-valued velocity vector, w, is defined to be $w = u + iv$. It is clear that the autospectrum for w^{+} is $P^{+}_{ww} = A^2$ and that for w^{-} it is $P^{-}_{ww} = C^2$. Thus, there is physical meaning for spectra with negative as well as positive frequencies. The total auto-spectrum for w is

$$P_{ww} = P^{+}_{ww} + P^{-}_{ww} = A^2 + C^2 = P_{uu} + P_{vv} .$$

It also follows that

$$P^{+}_{ww} - P^{-}_{ww} = (A^2 - C^2) = 2Q_{uv} .$$

Thus, P^{+}_{ww} and P^{-}_{ww} are invariant under coordinate rotation.

The two counter-rotating vectors corresponding to the hodograph of Figure 42a are shown in Figure 42b.

C. Spectral Quantities for Pairs of Complex-Valued Time Series.

For the study of the coherency of a pair of two-dimensional

velocity vectors, in addition to the component-wise coherence and phase matrices, there is a quantity which measures the overall coherency of two velocity vectors. In essence, the coherency of a pair of horizontal hodographs is considered. Each horizontal velocity vector series is written as a complex-valued series with real argument, t, i.e., $w(t) = u(t) + iv(t)$. The material of this section was derived in a search for a technique which would provide quantitative results which were invariant under coordinate rotation.

Autovariance and Autospectrum Functions. The autovariance function for w is defined as,

$$R_{ww}(\tau) = \overline{w(t)w^{*}(t+\tau)}^{\,t},$$

where $(\ )^{*}$ is the conjugate operator; in coordinate form,

$$R_{ww}(\tau) = [R_{uu}(\tau)+R_{vv}(\tau)]+i[R_{vu}(\tau)-R_{uv}(\tau)],$$

$$= [R_{uu}(\tau)+R_{vv}(\tau)]-i2Q_{uv}(\tau),$$

which is invariant under coordinate rotation by Section A. Then the autospectrum is

$$P_{ww}(\sigma) = \text{F.T.}(R_{ww}(\tau))$$

$$= [P_{uu}(\sigma)+P_{vv}(\sigma)] + 2Q_{uv}(\sigma),$$

which is also invariant. $P_{ww}(\sigma)$ is not an energy spectrum in the usual physical sense because it is two-sided; i.e. it is neither odd nor even as a function of frequency. The variance of w does equal

$$\int_{-\infty}^{\infty} P_{ww}(\sigma)d\sigma \quad .$$

Covariance and Cross Spectrum Functions. The covariance function for w_1 and w_2 is defined as

$$R_{w_1 w_2}(\tau) = \overline{w_1(t) w_2^*(t+\tau)}$$

$$= [R_{u_1 u_2}(\tau) + R_{v_1 v_2}(\tau)] + i[R_{v_1 u_2}(\tau) - R_{u_1 v_2}(\tau)].$$

When w_1 and w_2 undergo a coordinate transformation to w_1' and w_2' by a rotation through an angle of θ_1 and θ_2, respectively, it follows that

$$R_{w_1' w_2'}(\tau) = R_{w_1 w_2}(\tau)\, e^{i(\theta_2 - \theta_1)}.$$

Thus, the absolute value of the covariance function is invariant. The cross spectrum is

$$\tilde{P}_{w_1 w_2}(\sigma) = F.T.(R_{w_1 w_2}(\tau)) = P_{w_1 w_2}(\sigma) + iQ_{w_1 w_2}(\sigma),$$

where the cospectrum is

$$P_{w_1 w_2}(\sigma) = [P_{u_1 u_2}(\sigma) + P_{v_1 v_2}(\sigma)] - [Q_{v_1 u_2}(\sigma) - Q_{u_1 v_2}(\sigma)]$$

and the quadrature spectrum is

$$Q_{w_1 w_2}(\sigma) = [Q_{u_1 u_2}(\sigma) + Q_{v_1 v_2}(\sigma)] + [P_{v_1 u_2}(\sigma) - P_{u_1 v_2}(\sigma)].$$

The absolute value of the cross spectrum is invariant under

coordinate rotation from the above. The forms of $P_{w_1 w_2}(\sigma)$ and $Q_{w_1 w_2}(\sigma)$ contain terms accounting for the component-wise coupling of the two velocity vectors; these terms are the elements of the component-wise cross spectral matrix.

Coherence Squared and Phase Functions. The coherence squared, γ^2, and phase, Φ, are defined in the usual way, dropping the frequency argument, σ, for convenience :

$$\gamma^2_{w_1 w_2} = \frac{|\tilde{P}_{w_1 w_2}|^2}{P_{w_1 w_1} P_{w_2 w_2}}$$

$$= \frac{[P_{u_1 u_2} + P_{v_1 v_2} + Q_{u_1 v_2} - Q_{v_1 u_2}]^2 + [Q_{u_1 u_2} + Q_{v_1 v_2} + P_{v_1 u_2} - P_{u_1 v_2}]^2}{[P_{u_1 u_1} + P_{v_1 v_1} + 2Q_{u_1 v_1}][P_{u_2 u_2} + P_{v_2 v_2} + 2Q_{u_2 v_2}]}$$

and

$$\Phi_{w_1 w_2} = \tan^{-1}\left[\frac{Q_{w_1 w_2}}{P_{w_1 w_2}}\right]$$

$$= \tan^{-1} \frac{[Q_{u_1 u_2} + Q_{v_1 v_2} + P_{v_1 u_2} - P_{u_1 v_2}]}{[P_{u_1 u_2} + P_{v_1 v_2} + Q_{u_1 v_2} - Q_{v_1 u_2}]} .$$

By the preceding remarks, γ^2 is invariant under coordinate rotation and $\Phi'_{w_1' w_2'} = \Phi_{w_1 w_2} + (\theta_2 - \theta_1)$.

It remains to prove that $\gamma^2_{w_1 w_2}$ is bounded above by 1.0. The most instructive way to do this is to use a model for w_1 and w_2 composed of a sum of sinusoids in each hypothetical measurement bandwidth. Form w_1 and w_2 from a set of sinusoids :

$$u_1 = A_1 \cos(\sigma t) + B_1 \sin(\sigma t),$$

$$v_1 = C_1 \cos(\sigma t) + D_1 \sin(\sigma t),$$

$$u_2 = A_2 \cos(\sigma t) + B_2 \sin(\sigma t),$$

and

$$v_2 = C_2 \cos(\sigma t) + D_2 \sin(\sigma t),$$

thus

$$w_1 = \sum_k [(A_1^{(k)} \cos(\sigma_k t) + B_1^{(k)} \sin(\sigma_k t)) + i(C_1^{(k)} \cos(\sigma_k t) + D_1^{(k)} \sin(\sigma_k t))],$$

and similarly for w_2, where k is summed over the number of frequencies in a measurement bandwidth. Dropping the superscript k for convenience, it is straightforward to show that

$$P_{w_i w_j} = \frac{1}{2} \sum_k [(A_i + D_i)(A_j + D_j) + (B_i - C_i)(B_j - C_j)]$$

and

$$Q_{w_i w_j} = \frac{1}{2} \sum_k [(A_i + D_i)(B_j - C_j) - (A_j + D_j)(B_i - C_i)].$$

Now take

$$\underline{I}(k) = [(A_i + D_i), (B_i - C_i)]$$

and

$$\underline{J}(k) = [(A_j + D_j), (B_j - C_j)],$$

thus

$$P_{w_i w_j} = \frac{1}{2}[\sum_k \underline{I} \cdot \underline{J}] = \frac{1}{2} \sum_k |\underline{I}| \, |\underline{J}| \cos \Phi$$

and

$$Q_{w_i w_j} = \frac{1}{2}[\sum_k \underline{I} \times \underline{J}] = \frac{1}{2} \sum_k |\underline{I}| \, |\underline{J}| \sin \Phi,$$

where Φ is the angle between $\underline{I}(k)$ and $\underline{J}(k)$.

With use of the C-B-S inequality in summation form, it follows that

$$|\tilde{P}_{w_i w_j}|^2 = \frac{1}{4}\{[\sum_k |\underline{I}||\underline{J}| \cos \Phi]^2 + [\sum_k |\underline{I}||\underline{J}| \sin \Phi]^2\}$$

$$\leq \frac{1}{4}\{[\sum_k |\underline{I}|^2 (\sum_k |\underline{J}|^2 \cos^2 \Phi + \sum_k |\underline{J}|^2 \sin^2 \Phi)\}$$

$$= \frac{1}{4} \sum_k |\underline{I}|^2 \sum_k |\underline{J}|^2$$

$$= P_{w_i w_i}(\sigma) P_{w_j w_j}(\sigma).$$

Therefore,

$$\gamma^2_{w_i w_j}(\sigma) \leq 1.0 ;$$

the equality holds only when $\underline{I} = \underline{J}$ all k or when there is only one sinusoid in a measurement band. γ^2 and Φ for complex-valued series obey the same statistics as they do for real series. The equations for the cospectrum and quadrature spectrum are in the proper form for use in band-averaging a set of Fourier coefficients.

Since $P_{ww} = \frac{1}{2} \sum_k [(A+D)^2 + (B-C)^2]$, then $P_{ww} = 0$ if and only if $A^{(k)} = -D^{(k)}$ and $B^{(k)} = C^{(k)}$ for all k. Thus, when the denominator of γ^2 vanishes, the numerator also vanishes.

Degenerate Cases. If one series is complex, e.g., velocity, and a second real, e.g., temperature, set $w_1 = w = u + iv$ and $w_2 = s$. Then

$$P_{w_1 w_2} = P_{ws} = P_{us} - Q_{vs}$$

and

$$Q_{w_1 w_2} = Q_{ws} = Q_{us} + P_{vs} ,$$

thus

$$\gamma^2_{ws} = \frac{[P_{us} - Q_{vs}]^2 + [Q_{us} + P_{vs}]^2}{P_{ss}[P_{uu} + P_{vv} + 2Q_{uv}]}$$

and

$$Q_{ws} = \tan^{-1} \left(\frac{Q_{us} + P_{vs}}{P_{us} - Q_{vs}} \right) .$$

If both series are real, i.e., v_1 and $v_2 = 0$, then the above formulae reduce to the ordinary forms in the cross spectrum analysis of real-valued series.

The Complex Spectrum of a Pair of Hodographs. As seen in Section B, the hodograph can be reduced to components with positive and negative frequencies. The spectrum of the hodograph, Section B, for positive and negative frequencies is recognized as the spectrum of a complex-valued series as discussed above. The detailed steps are illustrated for a pair of hodographs. Take $u_1 = (A_1 + C_1) \cos(\sigma t + \theta_1)$ and $v_1 = (A_1 - C_1) \sin(\sigma t + \theta_1)$, then

$$w_1 = u_1 + iv_1 = [A_1 e^{i(\sigma t + \theta_1)} + C_1 e^{-i(\sigma t + \theta_1)}]$$

and an analogous form is used for w_2. Thus,

$$R_{w_1 w_1}(\tau) = A_1^2 e^{-i\sigma\tau} + C_1^2 e^{+i\sigma\tau} ,$$

$$R_{w_2 w_2}(\tau) = A_2^2 e^{-i\sigma\tau} + C_2^2 e^{i\sigma\tau} ,$$

and

$$R_{w_1 w_2}(\tau) = A_1 A_2 e^{-i(\sigma\tau-(\theta_1-\theta_2))} + C_1 C_2 e^{i(\sigma\tau-(\theta_1-\theta_2))} .$$

Then

$$P_{w_1 w_1}(\sigma_o) = A_1^2 \delta(\sigma-\sigma_o) + C_1^2 \delta(\sigma+\sigma_o) ,$$

$$P_{w_2 w_2}(\sigma_o) = A_2^2 \delta(\sigma-\sigma_o) + C_2^2 \delta(\sigma+\sigma_o) ,$$

and

$$\tilde{P}_{w_1 w_2}(\sigma_o) = A_1 A_2 \delta(\sigma-\sigma_o) e^{i(\theta_1-\theta_2)} + C_1 C_2 \delta(\sigma+\sigma_o)\, e^{-i(\theta_1-\theta_2)} ,$$

thus

$$\left|\tilde{P}_{w_1 w_2}(\sigma_o)\right|^2 = A_1^2 A_2^2 \delta(\sigma-\sigma_o) + C_1^2 C_2^2 \delta(\sigma+\sigma_o) ,$$

where $\delta(\ )$ is a Dirac delta function.

For a sum of sinusoids in a measurement band, the coherence squared is then

$$\gamma^2_{w_1 w_2} = \begin{cases} \dfrac{(\Sigma A_1 A_2)^2}{\Sigma(A_1)^2 \Sigma(A_2)^2} , & \sigma \geq 0 \\ \dfrac{(\Sigma C_1 C_2)^2}{\Sigma(C_1)^2 \Sigma(C_2)^2} , & \sigma \leq 0 . \end{cases}$$

Thus, there is a value of $\gamma^2_{w_1 w_2}$ defined for the anticlockwise $(\sigma \geq 0)$ portion of w_1 and w_2 and a value for the clockwise, $(\sigma \leq 0)$ portion. Several special cases exist for the spectrum of the hodograph :

i) $A = C$, $P_{ww}(-\sigma) = P_{ww}(\sigma)$, rectilinear motion,

ii) $C = 0$, $P_{ww}(-\sigma) = 0$, pure anticlockwise motion,

iii) $A = 0$, $P_{ww}(\sigma) = 0$, pure clockwise motion.

In general, $P_{ww}(-\sigma) < P_{ww}(\sigma)$ for net anticlockwise motion and vice versa for net clockwise motion.